Spin-forbidden $c\,^3\Sigma^+(\Omega = 1) \leftarrow X\,^1\Sigma^+$ transition in NaCs: Investigation of the $\Omega = 1$ state in hot and cold environments

A. Grochola and P. Kowalczyk
Institute of Experimental Physics, Faculty of Physics, University of Warsaw, ulica Hoża 69, PL-00-681 Warszawa, Poland

J. Szczepkowski and W. Jastrzebski
Institute of Physics, Polish Academy of Sciences, Aleja Lotników 32/46, PL-02-668 Warsaw, Poland

A. Wakim, P. Zabawa, and N. P. Bigelow
Department of Physics and Astronomy and Laboratory for Laser Energetics, University of Rochester, Rochester, New York 14627, USA
(Received 16 May 2011; published 18 July 2011)

Comprehensive spectroscopic studies of hot and ultracold samples of NaCs molecules were combined to complete the investigation of the $(3)\Omega = 1 \leftarrow X\,^1\Sigma^+$ transition for the NaCs molecule. Polarization labeling, photoassociation, and pulsed laser depletion spectroscopy were used to collect data on rovibrational levels of the $(3)\Omega = 1$ state [here described as the $c\,^3\Sigma^+$ state in Hund's case (a) notation]. The highest observed level was $v = 72$ located ~5 GHz below the atomic asymptote $\mathrm{Na}(3\,^2S_{1/2}) + \mathrm{Cs}(6\,^2P_{3/2})$. Approximately 1400 levels were used to construct the potential energy curve of the $(3)\Omega = 1$ state for the full range of interatomic distances.

DOI: 10.1103/PhysRevA.84.012507 PACS number(s): 33.20.Kf, 33.20.Vq, 42.62.Fi

I. INTRODUCTION

The majority of NaCs electronic states have not been experimentally determined. Only five states have been characterized, namely the two lowest states, $X\,^1\Sigma^+$ and $a\,^3\Sigma^+$ [1,2], and three excited states, $B(1)^1\Pi$, $D(2)^1\Pi$, and $3^1\Pi$ [1,3–6]. Further spectroscopic studies on additional electronic states are necessary to complete our understanding, to test *ab initio* theoretical predictions, and to facilitate experiments on the formation of ultracold NaCs molecules [7–11].

In this paper, we present a study of the $(3)\Omega = 1 \leftarrow X\,^1\Sigma^+$ transition. We have combined complementary data sets from two groups. Part of this data was obtained after our recent spectroscopic investigation of the $B \leftarrow X$ transition in NaCs [6]. A polarization labeling spectroscopy (PLS) experiment done in Warsaw provided an accurate potential energy curve of the $B\,^1\Pi$ state, nearly up to the dissociation limit. Over the course of that experiment, several levels in the B state were found to be perturbed, presumably by the neighboring $c\,^3\Sigma^+$ state levels, and some extra lines appeared in the spectra. By increasing the excitation laser energy, we increased the sensitivity of the experiment and were able to observe many more of these lines, forming a whole band system. We attribute the appearance of these lines to a nominally spin-forbidden transition from the ground electronic state of NaCs, $X\,^1\Sigma^+$, to the $\Omega = 1$ component of the $c\,^3\Sigma^+$ state, observable at conditions of our experiment even over a range where the transition probability is not enhanced by the $c\,^3\Sigma^+ \sim B^1\Pi$ mixing. It must be noted that at around $R = 6.5$ Å this state adiabatically becomes the $\Omega = 1$ component of the $b\,^3\Pi$ state and correlates to the $\mathrm{Na}(3\,^2S_{1/2}) + \mathrm{Cs}(6\,^2P_{3/2})$ atomic asymptote [12].

At the same time, an experiment performed in Rochester provided transitions to the highest vibrational levels of the same $\Omega = 1$ state observed via photoassociation (PA) spectroscopy of ultracold NaCs molecules in a dual-species magneto-optical trap. PA through this excited state populates deeply bound levels in the $X\,^1\Sigma^+$state. From this initial distribution, pulsed laser depletion spectroscopy was performed to acquire the $c\,^3\Sigma^+(\Omega = 1) \leftarrow X$ transition for low rotational levels. Joint analysis of the experimental data, collected both in hot and cold environments, enables us to determine a potential energy curve of the $\Omega = 1$ state to 0.17 cm^{-1} from the dissociation limit.

II. EXPERIMENT

A. Polarization labeling spectroscopy

The method for the Warsaw part of the experiment has been presented before [6,13], and therefore only a short summary of the important experimental details is given below. We employ the V-type optical-optical double-resonance polarization labeling spectroscopy technique with two independent pump and probe lasers. In our method, the probe laser has a fixed frequency and excites a few assigned molecular transitions while the pump laser is tuned over the investigated spectrum. The pump laser is a high-power optical parametric oscillator-amplifier system (Continuum, Sunlite EX) pumped with an injection seeded Nd:YAG laser (Powerlite 8000). The system delivers pulses up to 20 mJ energy, 10 ns duration, and 0.08 cm^{-1} spectral width. In the present experiment, spectra are recorded as the pump laser is tuned from 14300 to 16500 cm^{-1}. Calibration is provided by simultaneously recording the argon optogalvanic spectrum and monitoring fringes from a Fabry-Pérot interferometer. We estimate that the absolute frequency of the pump laser is determined with an accuracy of 0.05 cm^{-1}. The weaker, home-built probe dye laser (spectral width about 0.3 cm^{-1}, pumped synchronously by the same Nd:YAG laser) is operated with Coumarin 153 dye and set at selected rovibronic transitions in the $D\,^1\Pi \leftarrow X\,^1\Sigma^+$ system of NaCs, known from high-resolution measurements reported in the literature [1]. To set the probe laser frequency, we use a HighFinesse WS-7 wavemeter. The NaCs molecules

are prepared in a dual-temperature heat pipe oven [14] in the presence of 4 Torr of helium as a buffer gas. The copropagating pump and probe laser beams intersect in the central part of the oven at a small angle, providing an interaction length of a few centimeters. While tuning the pump beam over the investigated spectrum, the intensity of the probe beam is monitored through a polarizer-analyzer system (Glan-Thompson prisms, placed either side of the heat pipe), so the double-resonance signals appear on a black background. This method provides very high sensitivity to observe the excitation spectra of NaCs.

B. Photoassociation and pulsed laser depletion spectroscopy

The Rochester experiment started with a ~200-μK NaCs sample produced by PA from overlapped magneto-optical traps of sodium and cesium atoms. In the PA spectroscopy, a Ti-sapphire laser was scanned below the Cs $6\,^2P_{3/2}$ asymptote to locate the excited-state vibrational levels that were coupled in the electronic ground-state molecular formation process. Eleven vibrational levels were observed spanning 1000 GHz and were found to belong to the investigated $(3)\Omega = 1$ state. Spectra were taken with resolution of 20 MHz and absolute accuracy of ± 2 GHz, allowing the hyperfine structure of the rotational levels $J' = 1,2,3,4,5$ to be observed.

A PA resonance detuned ~32 GHz from the Cs $6\,^2P_{3/2}$ asymptote, belonging to the $B\,^1\Pi$ state, was employed to produce deeply bound singlet ground-state molecules in a range of vibrational levels, $X\,^1\Sigma^+(v'' = 4\text{–}34)$, in the lowest rotational levels, $J'' = 0,1$, and 2. From this initial distribution of rovibrational levels, pulsed laser depletion spectroscopy [11] (PDS) was used to obtain positions of the $(3)\Omega = 1$ vibrational levels. The PDS spectrum highlights specific transitions to the excited state by affecting the population in an initial vibrational level probed using resonance enhanced multiphoton ionization (REMPI). Prior to REMPI detection, the sample was depleted by a separate laser pulse (linewidth 0.6 cm^{-1}) that is resonant with a transition to an excited-state vibrational level and drives population out of the initial vibrational state. In this way, the PDS spectrum mapped the $c\,^3\Sigma^+(\Omega = 1) \leftarrow X$ transition with ~1 cm^{-1} accuracy.

III. RESULTS AND ANALYSIS

The Warsaw part of the experiment began with a survey of the $B\,^1\Pi \leftarrow X\,^1\Sigma^+$ system. As mentioned earlier, after increasing the pump laser intensity to saturate the $B \leftarrow X$ transition, another band system emerged in the spectrum (Fig. 1). The presence of P, Q, and R lines and their positions in frequencies suggest that these transitions are from the ground electronic state of NaCs to the $\Omega = 1$ component of the $c\,^3\Sigma^+$ state. Apparently the scheme of angular momentum coupling in the NaCs molecule is sufficiently close to Hund's case (c) that this transition is partially allowed and should be labeled as the $(3)\Omega = 1 \leftarrow X(1)\Omega = 0^+$ transition. The notation $(3)\Omega = 1$ refers to the third $\Omega = 1$ electronic state in the excitation energy scale, which is related adiabatically to the Hund's case (a) $c\,^3\Sigma^+$ state in the short-range part and to the $b\,^3\Pi$ state close to the asymptote. Therefore, we refer further to the $B \leftarrow X$ transition as the $(4)\Omega = 1 \leftarrow X(1)\Omega = 0^+$transition.

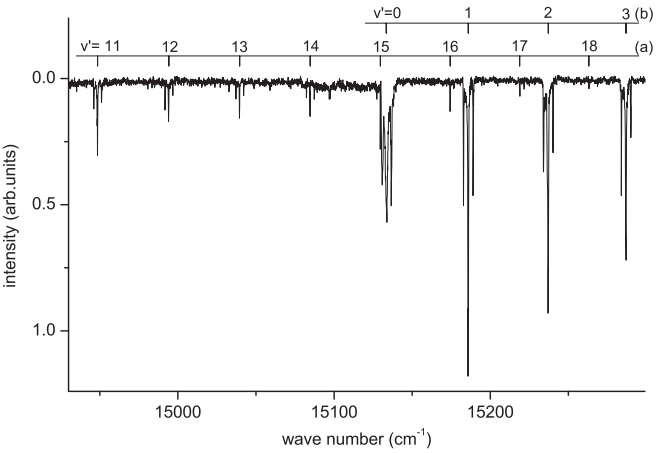

FIG. 1. A fragment of the polarization spectrum of NaCs. The progressions assigned on the top correspond to transitions $(3)\Omega = 1 \leftarrow X(1)\Omega = 0^+$ (a) and $B(4)\Omega = 1 \leftarrow X(1)\Omega = 0^+$ (b) from the ground state level $v'' = 2, J'' = 36$ labeled by the probe laser set at the wave number 18025.2 cm^{-1}. Note strong saturation of lines in the $B \leftarrow X$ system.

It is worth noting that the bottom of the $(3)\Omega = 1$ state is located more than 700 cm^{-1} below that of $B\,^1\Pi$ and therefore it is unlikely that the $(3)\Omega = 1$ state is made observable by $c\,^3\Sigma^+ \sim B\,^1\Pi$ spin-orbit mixing. Such a mixing does exist in a few energy ranges but is marked by a substantial increase of intensity of the $(3)\Omega = 1 \leftarrow X(1)\Omega = 0^+$ transitions and irregular positions of some spectral lines.

During the experiment, around 1300 transitions were assigned to the $(3)\Omega = 1 \leftarrow X(1)\Omega = 0^+$ system, originating from ground-state vibrational levels $v'' = 0 - 3$, sufficiently populated in our heat pipe source. The transitions span 61 vibrational levels in the $(3)\Omega = 1$ state with a good coverage of rotational quantum numbers $J' = 13\text{–}52$. The wave numbers of spectral lines were converted to energies of rovibrational levels by adding term values of the ground $X\,^1\Sigma^+$ state [1], resulting in an absolute accuracy better than 0.1 cm^{-1}. However, unfavorable Franck-Condon factors for transitions between the bottom of the ground-state potential to the lowest levels of the investigated $(3)\Omega = 1$ state did not allow us to establish an absolute vibrational numbering of the investigated state. The final numbering of vibrational levels had to be based on another measurement, described below.

There were two types of data provided by the Rochester experiment. The pulsed laser depletion spectroscopy method supplied transition energies from higher lying ground-state vibrational levels $v'' \geqslant 5$ to the $(3)\Omega = 1$ state (altogether 78 lines) measured with a precision of ~1 cm^{-1}. Although having relatively low influence on determination of molecular constants or molecular potential because of their lower absolute accuracy, these spectra allowed for direct determination of vibrational numbering in the $(3)\Omega = 1$ state, due to increased transition strengths for transitions to $v' = 0$ (Fig. 2). First, using data taken with an initial distribution of $X\,^1\Sigma^+$ ($v'' = 9$), the position of the presumably lowest vibrational level in the $(3)\Omega = 1$ state was obtained. To verify the location of the deepest vibrational level, some 10 000 GHz below the

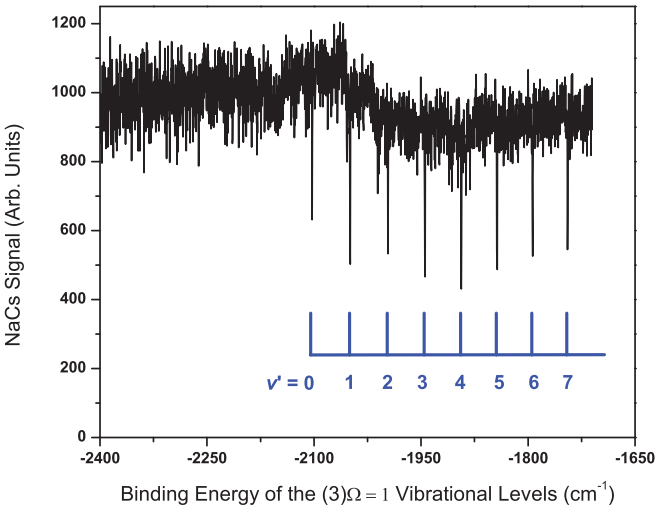

FIG. 2. An example of the pulsed laser depletion spectrum showing transitions from $v'' = 9$ in the ground state of NaCs to the lowest vibrational levels v' in the $(3)\Omega = 1$ state.

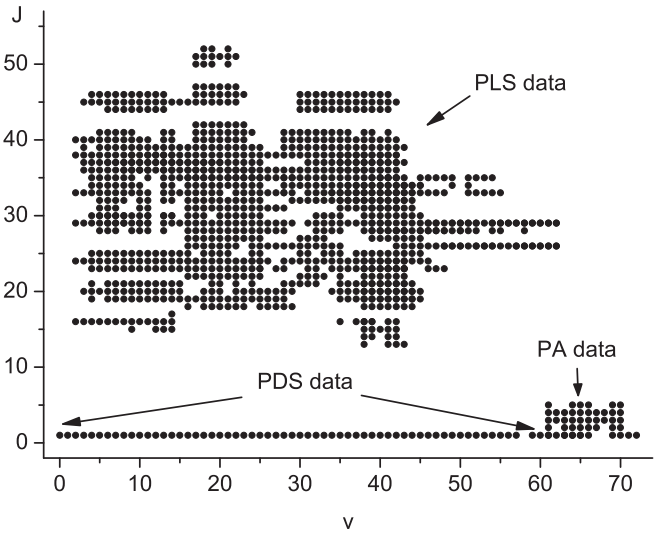

FIG. 3. Distribution of the experimental data in the field of vibrational and rotational quantum numbers of the $(3)\Omega = 1$ state of NaCs, observed by PLS, PDS, and PA.

last resonance were scanned with no indication of any other relevant transition. As confirmed later based on the calculated Franck-Condon factors, transition $v' = 0 \leftarrow v'' = 9$ should be strong and readily observable. Further, a PDS spectrum from the initial vibrational level of $X\,^1\Sigma^+$ ($v'' = 5$) to the lowest levels of the $(3)\Omega = 1$ state confirmed that there were no deeper vibrational levels. By combining spectra taken with various initial vibrational levels, $X\,^1\Sigma^+$ ($v'' = 13,15,19,21,23,25$), transitions to $v' = 0$–65 in the $(3)\Omega = 1$ state were located. On the other hand, the photoassociation spectroscopy provided positions of the near-dissociation excited vibrational levels with an accuracy of 0.06 cm^{-1} (limitation due to hyperfine structures of the observed lines), which supplied information about the highest part of the investigated state, corresponding to $v' = 61$–72, $J' = 1$–5 (43 resonances).

Figure 3 displays all the levels observed experimentally. Application of Dunham formalism to describe the $(3)\Omega = 1$ state turned out to be successful only for levels from $v' = 0$ to 25 (see Table I). The molecular constants relevant to this range reproduce the positions of energy levels of both e and f parities determined in the PLS experiment with a root-mean-square deviation of 0.05 cm^{-1}, in good agreement with accuracy achievable for unperturbed states in our past experiments. All the observed levels from this range have been incorporated into the fit. Levels above $v' = 25$ could only be included if many (ill-defined) coefficients were added to the Dunham expansion, although the potential well supports more than 70 levels. This is typical for electronic states characterized by potential curves with a shape differing from the Morse potential. Therefore, to describe the whole $(3)\Omega = 1$ state, we have chosen to construct the energy curve with the point-wise inverted perturbation approach (IPA) method [15] suitable for such cases. The method is based on iterative optimization of an approximate initial potential in a way that the calculated eigenenergies agree in a least-squares sense with the experimental term values. For the initial potential, we use the Rydberg-Klein-Rees potential generated from the Dunham coefficients of Table I and extended beyond the limits of its reliability to large interatomic distances, matched smoothly with a long-range part of the form

$$U(R) = U(\infty) - C_6/R^6 - C_8/R^8 - C_{10}/R^{10} \quad \text{for} \quad R > R_{\text{out}}, \tag{1}$$

with R_{out} denoting a matching point of the short-range and long-range parts. The energy of the atomic asymptote, relative to the bottom of the ground potential, was fixed at the value $U(\infty) = 16686.547$ cm^{-1}, resulting from the well-known distance between the $6\,^2S_{1/2}$ and $6\,^2P_{3/2}$ energy levels in cesium atom [16] and the ground-state dissociation energy of NaCs [2]. The C_6 and C_8 coefficients were taken initially from *ab initio* calculations by Bussery *et al.* [17] and then used as the fitting parameters. The C_{10} coefficient and the

TABLE I. The Dunham coefficients that describe the $(3)\Omega = 1$ state of NaCs in the range $0 \leqslant v' \leqslant 25$, $13 \leqslant J' \leqslant 51$. The number in parentheses that follows a quantity is the error of a constant (one standard deviation) given in units of the last digits. For some coefficients, more figures are displayed than are statistically significant, as this number is required to reproduce the measured transitions.

Constant	Value (cm^{-1})
T_e	14558.83(11)
Y_{10}	52.3973(718)
Y_{20}	0.030478(800)
Y_{30}	−0.052102(1939)
$Y_{40} \times 10^2$	0.3643(81)
$Y_{50} \times 10^3$	−0.1054(34)
$Y_{60} \times 10^5$	0.110(4)
Y_{01}	0.038787(23)
$Y_{11} \times 10^3$	−0.3589(32)
$Y_{21} \times 10^5$	0.543(11)
$Y_{02} \times 10^7$	−0.69(5)
$q \times 10^3$	0.143(3)
rms	0.050

TABLE II. Parameters defining the IPA potential energy curve of the $(3)\Omega = 1$ state of NaCs.

R (Å)	U (cm^{-1})	R (Å)	U (cm^{-1})
2.4	29727.2633	7.0	16036.9412
2.6	24990.4728	7.2	16133.2912
2.8	21864.2749	7.4	16208.9728
3.0	19683.9887	7.6	16271.9689
3.2	18124.4018	7.8	16325.4945
3.4	16830.7370	8.0	16374.4334
3.6	16124.0709	8.2	16417.0169
3.8	15737.4482	8.4	16453.6268
4.0	15242.0798	8.6	16489.0947
4.2	14882.2724	8.8	16518.6541
4.4	14653.4028	9.2	16563.2505
4.6	14568.7429	9.6	16593.7972
4.8	14558.4133	10.4	16633.5845
5.0	14618.7808	11.2	16653.6696
5.2	14705.5185	12.0	16665.7349
5.4	14812.0455	12.8	16672.9646
5.6	14937.3480	14.4	16680.2626
5.8	15077.0980	16.0	16683.4237
6.0	15226.6600	17.6	16684.7813
6.2	15388.4238	20.0	16685.6947
6.4	15561.1169	22.0	16686.2827
6.6	15738.3493	25.0	16686.1716
6.8	15908.8198		
$R_{out} = 13.02151$ Å			
$U(\infty) = 16686.547\ cm^{-1}$			
$C_6 = 2.66558 \times 10^7\ cm^{-1}Å^6$		$C_8 = 8.17195 \times 10^9\ cm^{-1}Å^8$	
$C_{10} = -4.50611 \times 10^{11}\ cm^{-1}Å^{10}$			

point of connection R_{out} were chosen to ensure a smooth matching of the long-range and short-range potentials (with R_{out} confined to an interval of 13–14 Å consistent with the modified LeRoy radius [18] at 13.5 Å), and therefore these numbers have no physical meaning. As a fitting strategy, we adjust the short-range parameters (i.e., the set of points defining the potential) and the long-range parameters (C_n coefficients) in consecutive, separate runs of the IPA routine. Over the course of these fits, we have noticed that some rovibrational levels corresponding to $v' > 25$ are apparently perturbed as their energies deviate from the values predicted from the fitted IPA potential by more than two experimental uncertainties. Therefore, the final potential energy curve was generated using the robust fitting method proposed by Watson [19] where in subsequent iterations of the fit, each level i is weighted

$$w_i = \frac{1}{\sigma_i^2 + \alpha r_i^2}, \tag{2}$$

where σ_i is the experimental uncertainty and r_i is the residual from previous iteration. The value of the positive constant α, which controls the influence of the residuals on corresponding weights, has been chosen as 0.3 according to Watson's recommendation [19]. After performing several iterations, the statistical weights of levels that systematically deviate from the calculated positions are diminished according to their residuals. In our opinion, the potential curve constructed in this way is a closer approximation to the perturbation-free one than any curve based on a limited data set with some levels arbitrarily excluded as "perturbed." The results are summarized in Table II. The constructed potential is defined by the 45 points and the long-range coefficients listed there. In order to interpolate the potential to any middle point between 2.4 Å and R_{out}, the natural cubic spline should be used with all the grid points given in Table II. The numerical potential reproduces the experimental energies of 1415 rovibrational levels in the $(3)\Omega = 1$ state with a dimensionless standard error of 0.85, when the radial Schrödinger equation is solved in a mesh of at least 10000 points between 2.4 and 50 Å. For the e parity levels, the Λ doubling correction of the form $q_e J(J+1)$ has to be added. The highest level observed in the PA experiment ($v' = 72$, $J' = 1$) is located by 4.93 GHz below the atomic asymptote and has the classical outer turning point for vibrational motion at 24.8 Å.

It should be mentioned that when in the PLS experiment the pump laser was operated with sufficiently high power, in the spectral region covering the last 400 cm^{-1} below the atomic asymptote $Na(3\,^2S_{1/2}) + Cs(6\,^2P_{3/2})$, another, very weak band system could be detected, converging to the same limit as the $(3)\Omega = 1 \leftarrow X$ and $B(4)\Omega = 1 \leftarrow X$ systems. The presence of P, Q, and R lines in the extra system leads us to the somewhat surprising conclusion that we observe transition to the only remaining state with $\Omega \geqslant 1$ associated with this asymptote, that is, the $(1)\Omega = 2$ state [12]. The forbidden transition $(1)\Omega = 2 \leftarrow X(1)\Omega = 0^+$ apparently gains some intensity due to a mixing of the $(1)\Omega = 2$ state with the two neighboring $\Omega = 1$ states close to their common atomic

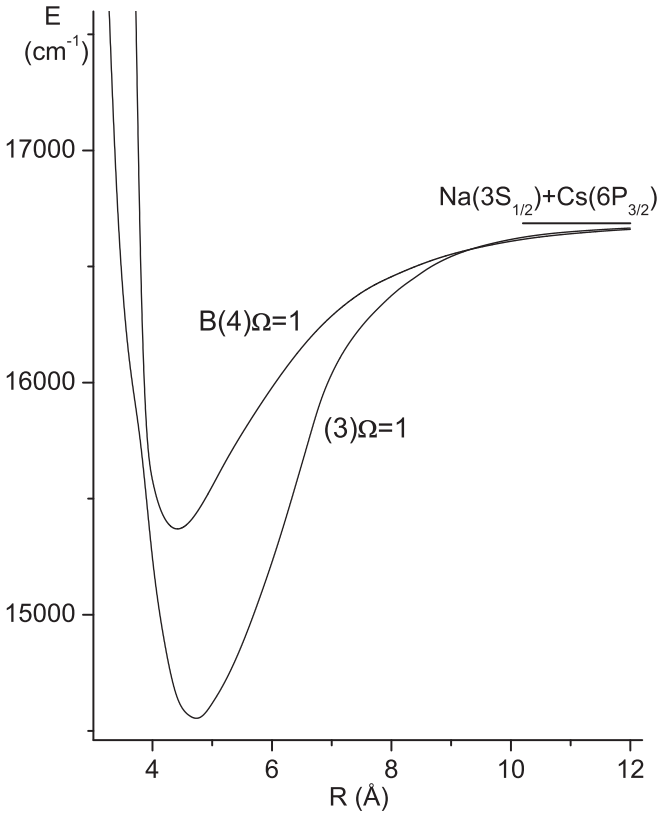

FIG. 4. The experimental potential curves of the $(3)\Omega = 1$ state (from the present work) and the $B(4)\Omega = 1$ state (from [6]).

asymptote. The same state was reported before in the PA spectra [9]. Unfortunately, the scarcity of the observed spectral lines and lack of information about the bottom of the $(1)\Omega = 2$ state did not allow us to pursue its analysis.

IV. SUMMARY REMARKS

To conclude, we have investigated the $(3)\Omega = 1$ state in NaCs from the very bottom of the molecular potential up to the dissociation limit by combining complementary data obtained with "cold" and "hot" molecular spectroscopy to yield a more complete potential energy curve than could be determined by either method separately.

We propose two different methods for the representation of rovibrational levels in the investigated $(3)\Omega = 1$ state. In the range $v' = 0$–25 they are described by a standard Dunham expansion (Table I). However, the whole range of the investigated levels can be represented only by the potential energy curve of Table II. The reason for that becomes clear when the $(3)\Omega = 1$ state potential is drawn alongside that of the $B(4)\Omega = 1$ state [6]. An avoided crossing of both curves at $R \approx 3.9$ Å is clearly visible (Fig. 4), and this distortion of the potentials prevents any effort to describe them globally even by a high-order polynomial. Note that both potentials come together again close to the dissociation limit and cross at $R \approx 9.3$ Å. This behavior can be viewed in two equivalent ways: diabatic, with crossing curves, or adiabatic, when they display an anticrossing. In our previous PLS experiment on the $B\,^1\Pi$ state [6], done at lower pump laser intensity, we were able to observe only one progression of vibrational levels converging to the atomic asymptote and assigned them to the B state. As a result of our present analysis, it turns out that this corresponds to the diabatic description of the $B(4)\Omega = 1$ state in the asymptotic region. To be consistent, we follow also the $(3)\Omega = 1$ state diabatically toward the asymptote, which results in crossing of the two related potentials.

TABLE III. Comparison of the experimental and theoretical [12] molecular constants (in cm^{-1} except for R_e in Å) for the $(3)\Omega = 1$ (present work) and $B(4)\Omega = 1$ [6] states in NaCs.

	$(3)\Omega = 1$		$B(4)\Omega = 1$	
Constant	Experiment	Theory	Experiment	Theory
T_e	14558.83	14687	15369.83	15430
ω_e	52.40	57.40	54.77	59.08
B_e	0.038787	0.0417	0.04402	0.0467
R_e	4.735	4.537	4.42	4.290

Finally, we compare the experimental molecular constants of the $(3)\Omega = 1$ and $B(4)\Omega = 1$ states with theoretical values resulting from *ab initio* calculations of Korek *et al.* [12]. The comparison is shown in Table III. The calculations place the bottoms of both potentials slightly too high (by 128 and 60 cm^{-1}, respectively) and overestimate the vibrational and rotational constants by not more than 10%. This shows reliability of modern *ab initio* methods even for many electron systems, although their results still lag far behind precision attainable in experiments.

ACKNOWLEDGMENTS

We acknowledge partial support received from the Polish Ministry of Science and Higher Education (Grant No. N202 203938) and from the European Regional Development Fund under the Operational Programme Innovative Economy. We are also grateful for funding provided by the US NSF and ARO.

[1] U. Diemer, H. Weickenmeier, M. Wahl, and W. Demtröder, Chem. Phys. Lett. **104**, 489 (1984).
[2] O. Docenko, M. Tamanis, J. Zaharova, R. Ferber, A. Pashov, H. Knöckel, and E. Tiemann, J. Phys. B **39**, S929 (2006).
[3] O. Docenko, M. Tamanis, J. Zaharova, R. Ferber, A. Pashov, H. Knöckel, and E. Tiemann, J. Chem. Phys. **124**, 174310 (2006).
[4] J. Zaharova, O. Nikolayeva, M. Tamanis, M. Auzinsh, R. Ferber, A. Zaitsevskii, E. A. Pazyuk, and A. V. Stolyarov, J. Chem. Phys. **124**, 184318 (2006).
[5] J. Zaharova, O. Docenko, M. Tamanis, R. Ferber, A. Pashov, H. Knöckel, and E. Tiemann, J. Chem. Phys. **127**, 224302 (2007).

[6] A. Grochola, P. Kowalczyk, and W. Jastrzebski, Chem. Phys. Lett. **497**, 22 (2010).
[7] C. Haimberger, J. Kleinert, M. Bhattacharya, and N. P. Bigelow, Phys. Rev. A **70**, 021402 (2004).
[8] C. Haimberger, J. Kleinert, O. Dulieu, and N. P. Bigelow, J. Phys. B **39**, S957 (2006).
[9] C. Haimberger, J. Kleinert, P. Zabawa, A. Wakim, and N. P. Bigelow, New. J. Phys. **11**, 055042 (2009).
[10] C. Haimberger, Ph.D. thesis, University of Rochester, 2010.
[11] P. Zabawa, A. Wakim, A. Neukirch, C. Haimberger, N. P. Bigelow, A. V. Stolyarov, E. A. Pazyuk, M. Tamanis, and R. Ferber, Phys. Rev. A **82**, 040501(R) (2010).
[12] M. Korek, S. Bleik, and A. R. Allouche, J. Chem. Phys. **126**, 124313 (2007).
[13] A. Grochola, W. Jastrzebski, P. Kortyka, and P. Kowalczyk, J. Mol. Spectrosc. **221**, 279 (2003).
[14] V. Bednarska, I. Jackowska, W. Jastrzebski, and P. Kowalczyk, Meas. Sci. Technol. **7**, 1291 (1996).
[15] A. Pashov, W. Jastrzebski, and P. Kowalczyk, Comput. Phys. Commun. **128**, 622 (2000).
[16] T. Udem, J. Reichert, T. W. Hänsch, and M. Kourogi, Phys. Rev. A **62**, 031801 (2000).
[17] B. Bussery, Y. Achkar, and M. Aubert-Frécon, Chem. Phys. **116**, 319 (1987).
[18] B. Ji, C.-C. Tsai, and W. C. Stwalley, Chem. Phys. Lett. **236**, 242 (1995).
[19] J. K. G. Watson, J. Mol. Spectrosc. **219**, 326 (2003).